Dual-Functionalized Crescent Microgels for Selectively Capturing and Killing Cancer Cells

Liu, Qian; Yuan, Zhenyu; Guo, Xuhong; van Esch, Jan H.

DOI
10.1002/anie.202005034

Publication date
2020

Document Version
Accepted author manuscript

Published in
Angewandte Chemie - International Edition

Dual-Functionalized Crescent Microgels for Selectively Capturing and Killing Cancer Cells

Qian Liu, [a] Zhenyu Yuan, [a] [b] Xuhong Guo[b] and Jan H. van Esch*[a]

Dedication

[a] Dr. Q. Liu, Dr. Z. Yuan, Prof. Dr. J. H. van Esch
Department of Chemical Engineering
Delft University of Technology
van der Maasweg 9, Delft, 2629 HZ, The Netherlands
E-mail: j.h.vanesch@tudelft.nl
[b] Dr. Z. Yuan, Prof. Dr. X. Guo
Department of Chemical Engineering
East China University of Science and Technology
Meilong 130, Shanghai, 200237, P. R. China

Supporting information for this article is given via a link at the end of the document.

Abstract: In cancer therapy, the selective targeting of cancer cells while avoiding side effects to normal cells is still full of challenges. Here, we developed dual-functionalized crescent microgels, which selectively captured and killed lung cancer cells in situ without killing other cells. Crescent microgels with the inner surface of the cavity functionalized with antibody and containing glucose oxidase (GOX) in the gel matrix have been produced in a microfluidic device. These microgels presented high affinity and good selectivity to lung cancer cells and retained them inside the cavities for extended periods of time. Exposing the crescent hydrogels to physiological concentrations of glucose leads to the production of a locally high concentration of H_2O_2 inside the microgels' cavities, due to the catalytic action by GOX inside the gel matrix, which selectively killed 90% cancer cells entrapped in the microgel cavities without killing the cells outside. Our strategy to create synergy between different functions by incorporating them in a single microgel presents a novel approach to therapeutic systems, with potentially broad applications in smart materials, bioengineering and biomedical fields.

Cancer is one of the leading health problems worldwide causing morbidity and mortality[1]. To cure cancer and inhibit tumor recurrence, chemotherapy with anti-cancer drugs is the relatively mature and most successful approach so far[2]. However, administration of conventional anti-cancer drugs is accompanied by strong side effects because the drug is not only cytotoxic to pathological tissues but also to healthy tissues[3]. A particular promising strategy to overcome these issues is the in-situ generation of therapeutic cytotoxins in or near pathological tissues. For instance, the in-situ generation of reactive oxygen species (ROS, like hydrogen peroxide (H_2O_2), superoxide anion radical ($^{\cdot}O^{2-}$) and the highly hydroxyl radical ($^{\cdot}OH$)), can induce cells apoptosis and/or necrosis by oxidative damages to cellular components, like DNA, proteins and lipids[4]. In healthy cells, ROS species are generated by aerobic metabolic processes and at normal levels do not lead to irreversible damage[5]. Cancer cells, however, are more susceptible to ROS than healthy cells because of their higher metabolic activity leading to the accumulation of high levels of ROS[6]. Therefore, the in-situ generation of ROS in or near cancer cells presents great potentials for effectively preventing side effects and selective cancer chemotherapy[7].

To produce high concentrations of ROS to kill cancer cells, a common strategy is by ROS-generating systems like photosensitizers using light[8] or oxidative enzymes in combination with their natural substrate[9] to produce ROS from molecular oxygen. Among them, glucose oxidase (GOX) has been widely used in cancer therapy due to its biocompatibility, high efficiency and absence of cytotoxic side effects, and because it generates ROS by catalytic oxidation of glucose[10]. Administration of GOX for ROS-mediated approaches has been achieved by e.g. loading GOX into various nano/microparticles, which after cellular uptake led to an increased cellular level of H_2O_2 and killing the host cell[11]. However, the lack of selectivity and specificity of these materials to cancer cells and the side effects of ROS on normal cells are still a serious challenge for the precise cancer therapy. Therefore, new strategies that enable the local generation of ROS and selective induction of cancer cell death are of great interest for biomedical engineering and clinical medicine.

In this study, we designed and fabricated antibody and GOX dual-functionalized crescent microgels. These microgels selectively captured lung cancer cells due to the asymmetric functionalization of the inner surface with antibody and locally produced a high level of H_2O_2 under the catalytic oxidation of physiological concentrations of glucose by GOX encapsulated in the gel matrix, which selectively killed the cancer cells inside the cavities without harming outside cells. Our strategy to create synergy between different functions by incorporating them in a single microgel presents a novel approach to therapeutic systems, with potentially broad applications in smart materials, bioengineering and biomedical fields.

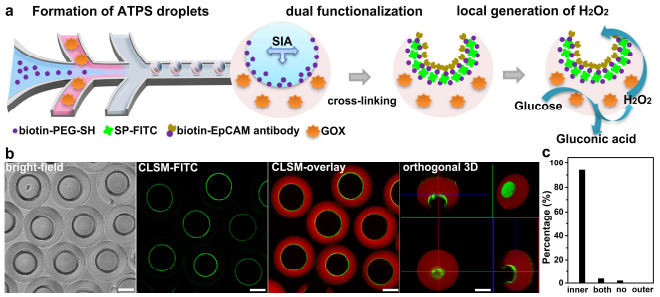

Figure 1. Fabrication of dual-functionalized crescent microgels. a, Schematic of the fabrication of dual-functionalized crescent microgels in a microfluidic device and their local generation of H_2O_2 based on the catalytic oxidation of glucose by GOX. **b**, Bright-field microscope image, confocal laser scanning microscope (CLSM) images of the dual-functionalized crescent microgels. Orthogonal images in x-y, x-z and y-z planes were shown, along with a 3D image. **c**, The distribution of streptavidin modification of ~200 microgels. The microgels were labelled by rhodamine B (red) and streptavidin were labelled by fluorescein isothiocyanate (FITC, green). Scale bar 50 μm.

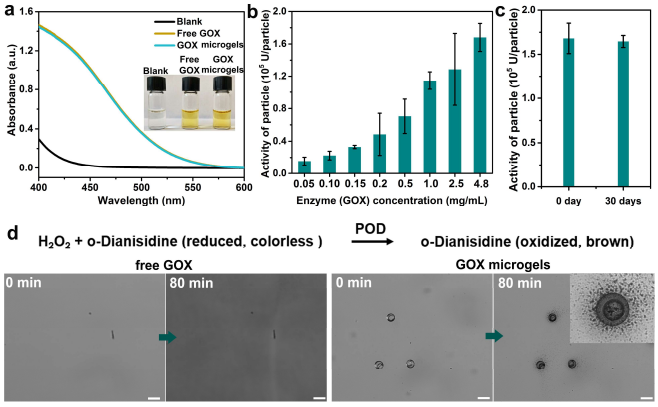

Figure 2. Local generation of H_2O_2 in the dual-functionalized crescent microgels. a, Absorbance spectra and color change (insert) of the solution without and with free GOX and dual-functionalized microgels in the gluconic acid-specific assay. 10 μg/mL free GOX, ~200 particles, 100 mM glucose, 100 mM hydroxylamine and 16 mM Fe^{3+} were used in this assay. **b**, Catalytic activity of the dual-functionalized microgels encapsulated with different concentrations of GOX. **c**, Stability of GOX in the dual-functionalized microgels after 30 days in PBS buffer solution. **d**, Visualization of the generation and distribution of H_2O_2 in the solution with free GOX (left) and dual-functionalized microgels (right, GOX=0.2 mg/mL) through oxidation reaction of *o*-dianisidine. These results are shown as the mean±s.d. of three independent experiments, with ~200 particles for each experiment. Scale bar 200 μm.

Crescent microgels were prepared by crosslinking of the photo-polymerizable poly(ethylene glycol)diacrylate (PEGDA) phase and removal of the nonpolymerizable dextran phase in phase-separated droplets generated in a microfluidic device[12]. Dual functionalization of the microgels was achieved by encapsulation of GOX in the gel matrix upon polymerization, with simultaneous asymmetric functionalization by selective interfacial accumulation (SIA) of biotin labels of the particle inner surface. As shown in **Figure 1a**, phase-separated droplets were obtained in the water-water-oil microfluidic device by injecting an aqueous two-phase systems (ATPS) of dextran and PEGDA into an oil phase. Biotin-PEG-thiol polymer (biotin-PEG-SH) was added to the dextran phase while GOX was added to the PEGDA phase. Previously we found that these biotin-PEG-SH polymers selectively accumulated in the interfacial layer between the two aqueous phases and could be immobilized on this interface by fast photo-cross-linking of PEGDA phase[13]. The photo-cross-linking reaction simultaneously leads to encapsulation of GOX in PEGDA gel matrix. Suspension of the polymerized microgels in water leads to dissolution and removal of the unpolymerized dextran phase, and GOX-encapsulated crescent microgels with the asymmetric functionalization of biotin-PEG-SH on their inner surface were obtained. The microgels' inner surface was further modified by sequentially reacting these microgels with streptavidin-fluorescein isothiocyanate (SP-FITC) and biotin-EpCAM antibody specific for epithelial cellular adhesion molecule (EpCAM, a marker for a variety of cancers[14]).

The dual-functionalized crescent microgels were characterized by a confocal laser scanning microscope (CLSM). As shown in **Figures 1b, 1c** and **Figure S2**, the microgels presented uniform size (diameter: 136±3 μm and opening size: 75±4 μm) and well-defined crescent morphology with preferred orientation of cavity facing upwards after sedimentation in aqueous solution[15]. The CLSM images and their statistical analysis indicate that around 92% gel particles were present SP-FITC signal (green) only on their inner surface. This result indicates that only the inner surface of crescent microgels is modified with the streptavidin label, thereby providing a handle to further selective functionalization of the cavity interior surface with EpCAM antibody *via* biotin-streptavidin interactions.

The presence of GOX in the crescent microgels was verified by the gluconic acid-specific assay[16]. As shown in **Figure 2a** and **Figure S3**, after reacting the microgels solution with hydroxylamine and subsequently binding of Fe^{3+}, the solution changed from colorless to yellow, with an increased absorbance from 450 to 525 nm. It reveals the generation of gluconic acid and the successful encapsulation of GOX in the microgels. The catalytic activities of these microgels were adjusted by varying the concentrations of GOX in the PEGDA solution. Different catalytic activities ranging from 0.15-1.68*10^{-5} units/particle have been achieved (**Figure 2b** and **SI section 6**). Also, the stability of GOX in these dual-functionalized microgels was evaluated. As shown in **Figure 2c**, after 30 days, the microgels' catalytic activity still amounted to ~1.65*10^{-5} U/particle, indicating that these GOX encapsulated within the hydrogel matrix has excellent stability.

To investigate the spatial distribution of H_2O_2 generated by encapsulated GOX, we exploited the oxidation of *o*-dianisidine by H_2O_2. The oxidation of *o*-dianisidine by H_2O_2 in aqueous solution leads to the formation of a brown-colored species that precipitates at higher concentration[17]. As shown in **Figure 2d** and **Supporting Video**, in the free GOX solution a brown color developed homogeneously and gradually increased over time. However, for the microgels with encapsulated GOX the brown precipitates were mainly generated within the microgel cavities and around the microgel particles. To further quantify the H_2O_2 concentration produced inside and outside the microgels, we utilized the relationship between the gray vale of the generated brown-colored *o*-dianisidine and the concentration of H_2O_2. As shown in **Figure S4**, for the microgels encapsulated with 0.2 mg/mL GOX, the concentration of H_2O_2 inside the microgels was higher than 1 mM whereas the concentration outside was tens to hundreds μM at different concentrations of glucose. These results clearly show that the dual-functionalized crescent microgels locally produce a high level of H_2O_2 in their cavities due to the encapsulation of GOX.

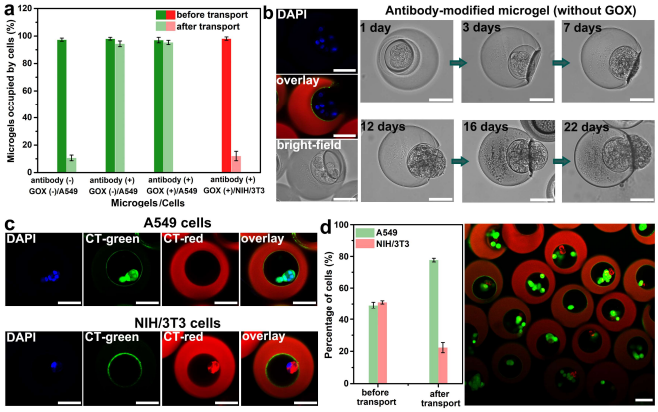

Figure 3. Selectivity of the dual-functionalized crescent microgels to cancer cells. a, Percentage of the microgels occupied by cells without (-) and with (+) the functionalization of antibody and GOX (0.2 mg/mL) before and after transport. A549 and NIH/3T3 cells were separately loaded into the microgels and cultured for 1 day in the growth medium without glucose. **b**, A549 cells inside the antibody-modified crescent microgels (without GOX) and their proliferation after transport. The cell nucleus was stained by DAPI (blue). **c**, Dual-functionalized microgels loaded with A549 cells (stained by CellTrackerTM green, CT-green) and NIH/3T3 Cells (stained by CellTrackerTM red, CT-red). **d**, Statistics of the percentage of A549 (green) and NIH/3T3 (red) cells co-cultured in the microgels before and after transport, and the corresponding CLSM image after transport. After transport the microgels with cells were cultured for 1 day in the growth medium without glucose. These results are shown as the mean±s.d. of three independent experiments, with ~200 particles for each experiment. Scale bar 50 μm.

To explore the application of the antibody and GOX dual-functionalized crescent microgels in cancer therapy, the selectivity of these microgels for binding of different types of cells was investigated. Various crescent microgels without and with functionalization of EpCAM antibody and GOX were fabricated and loaded with lung cancer cells (A549, EpCAM-positive cell line) and fibroblast cells (NIH/3T3, EpCAM-negative cell line). As shown in **Figure 3a** and **Figure S5**, around 98% of the microgel cavities were loaded with cells directly after sedimentation of the cells due to their preferred orientation[15]. After transporting the microgels to a different culture plate, only the microgels which were functionalized with EpCAM antibody retained the A549 cells, while microgels without antibody functionalization lost the cells after transport. In contrast, when the microgels were loaded with NIH/3T3 cells, 90% of the microgels lost the cells after transport, regardless whether they were modified with EpCAM antibody or not. These experiments clearly show that the lung cancer cells are strongly bound within the microgel cavities, most likely due to the immobilization of EpCAM antibody in the crescent microgels' cavities. After transport, the A549 cells inside the antibody-modified crescent microgels (without GOX) were further examined. As shown in **Figure 3b, Figures S6** and **S7**, the number of A549 cells entrapped in the microgel's cavity increased during culturing for 22 days due to cell proliferation, and after which the cavities became too small to accommodate all cells leading to their collective expulsion from the cavity. These results show that single-functionalized microgels with only antibody can retain the lung cancer cells inside their cavities for a prolonged period of time, but can't kill them.

To further investigate the selectivity of the microparticle cavities lined with EpCAM antibody, the dual-functionalized microgels were simultaneously loaded with A549 and NIH/3T3 cells, and further co-cultured in the growth medium without glucose. As shown in **Figures 3c**, **3d** and **Figure S8**, A549 and NIH/3T3 cells were stained by green and red probes, respectively. Directly after mixing the two types of cells with a ratio around 1:1 and loading into the microgels, the ratio of A549 and NIH/3T3 cells in the cavity was around 1:1 (49 % of A549 and 51 % of NIH/3T3). After transport and culturing for 1 day, the proportion of A549 cells increased to 77.7 % and that of NIH/3T3 decreased to 22.3 %. These experiments reveal that the dual-functionalized microgels screened the A549 cells, most likely due to the specific binding to the EpCAM antibody, and removed most unbound NIH/3T3 cells.

To investigate whether the local generation of high concentration of H_2O_2 can selectively kill cancer cells, different concentrations of GOX (0 to 4.8 mg/mL) were encapsulated in the dual-functionalized crescent microgels, following by loading with A549 cells inside and outside of the microgels. The cell viability inside and outside of the microgels were separately checked after culturing for 1 day. As shown in **Figure 4a, Figures S10** and **S11**, the cell viability both inside and outside of the particles were around 98% in the absence of GOX. It confirms that single-functionalized microgels can't kill the cancer cells. With the encapsulation of GOX increasing from 0.1 to 0.2 mg/mL, the outside cell viability stabilized at above 91%, whereas the inside cell viability decreased from 93% to 11% due to the increase of H_2O_2 concentration from several μM to ~1 mM. When the GOX was further increased from 0.2 to 4.8 mg/mL, all encapsulated cells were dead and the cell viability outside the cavities decreased from 91% to 0. These experiments show that for the dual-functionalized microgels, the modification with antibodies leads to the selective capturing of lung cancer cells and retains them in the cavity, giving the encapsulated GOX sufficient time to kill them, without killing other cells outside.

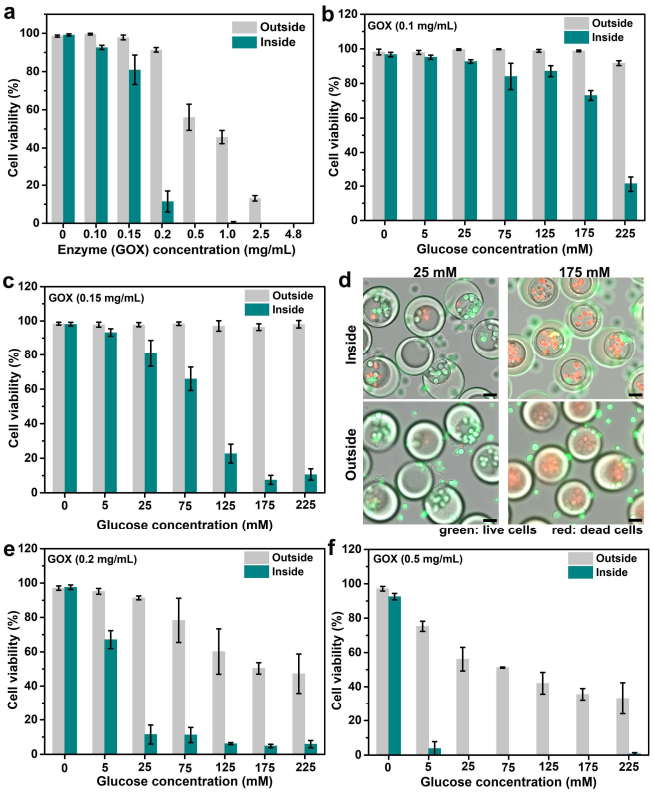

Figure 4. Selective killing of cancer cells by the dual-functionalized crescent microgels. **a**, Cell viability inside and outside of the microgels with

the encapsulation of different concentrations of GOX (the glucose in the cell culture medium was 25 mM). A549 cells were loaded inside and outside of the crescent microgels. At different glucose concentrations (from 0 to 225 mM), inside (emphasizing focus on the cells in the cavity) and outside (emphasizing focus on the cells at the culture plate bottom) cell viabilities of the microgels which were encapsulated with 0.1 (**b**), 0.15 (**c**) with the corresponding fluorescence images during the live/dead assay (**d**), and 0.2 (**e**), as well as 0.5 (**f**) mg/mL of GOX. These results are shown as the mean±s.d. of three independent experiments, with about 200 particles for each experiment. Cell viability was checked by the live/dead assay after varying the glucose concentration and culturing for 1 day. Calcein AM and propidium iodide (PI) were used to stain viable (green) and dead (red) cells, respectively. Scale bar 50 μm.

To further examine the efficacy of the dual-functionalized gels in selectively killing cancer cells under around physiological conditions, we explored the effect of different glucose concentrations on the fate of encapsulated cells and free cells outside the microgels. As shown in **Figures 4b, 4c, 4d** and **Figure S12**, microgels were encapsulated with 0.1 and 0.15 mg/mL of GOX, respectively. With the glucose concentration increasing from 0 to 225 mM, most cells outside stayed alive with a cell viability above 93%, while the viability of the cells inside the cavities gradually decreased from ~96% to ~8%. For the microgels with higher concentrations of GOX (0.2 and 0.5 mg/mL), as shown in **Figures 4e** and **4f**, cells inside the microgels only survived at very low concentration of glucose or no glucose. With the increase of glucose concentration, most inside cells were dead and the outside cell viability decreased to around 40%. Similar results have been achieved when A549 cells were loaded inside and NIH/3T3 cells were outside (**Figure S14**). These results indicate that the cancer cells which are captured inside the dual-functionalized microgels can be selectively and precisely killed in situ through varying the concentration of glucose without killing the cells outside.

In conclusion, we demonstrated a strategy of creating synergy by incorporating multiple functions in a single particle. Antibody and GOX dual-functionalized crescent microgels have been constructed, and applied for selectively capturing and killing cancer cells. Dual-functionalized crescent microgels were produced in the microfluidic device by asymmetric surface modification with biotin groups and encapsulating GOX inside the gel matrix, followed by functionalizing with EpCAM antibody. These dual-functionalized microgels presented high affinity and good selectivity to the lung cancer cells, which specifically trapped the cancer cells inside their cavities. Under the catalytic oxidation of glucose by GOX, a locally high concentration of H_2O_2 has been produced in their cavities, which selectively killed the cancer cells inside the microgels without harming the cells outside. Cells fate inside and outside of the microgels can be selectively and precisely controlled by varying the concentration of GOX and glucose. These synergic actions of two different functions within a single crescent microgel particle provide a new platform for selective cancer chemotherapy and hold great potential for applications in smart materials, biomedicine, and cancer therapy.

Acknowledgements

The authors gratefully acknowledge Dr. Serhii Mytnyk (Delft University of Technology) for design the microfluidic wafer and Dr. Meng Zhao (Delft University of Technology) for the suggestion of quantifying the H_2O_2 concentration inside and outside the microgels.

Keywords: microgels • synergy of multi-functions • cancer cell screening • selective cell therapy

[1] J. Ferlay, I. Soerjomataram, R. Dikshit, S. Eser, C. Mathers, M. Rebelo, D. M. Parkin, D. Forman, F. Bray, *Int. J. Cancer* **2015**, *136*, E359- E386.

[2] a) V. T. DeVita, E. Chu, *Cancer Res.* **2008**, *68*, 8643-8653; b) T. N. Chonghaile, K. A. Sarosiek, T.-T. Vo, J. A. Ryan, A. Tammareddi, V. D. G. Moore, J. Deng, K. C. Anderson, P. Richardson, Y.-T. Tai, C. S. Mitsiades, U. A. Matulonis, R. Drapkin, R. Stone, D. J. DeAngelo, D. J. McConkey, S. E. Sallan, L. Silverman, M. S. Hirsch, D. R. Carrasco, A. Letai, *Science* **2011**, *334*, 1129-1133.

[3] a) V. Sahni, D. Choudhury, Z. Ahmed, *Nat. Rev. Nephrol.* **2009**, *5*, 450-462; b) K. Cheng, X.-Q. Yang, X.-S. Zhang, J. Chen, J. An, Y.-Y. Song, C. Li, Y. Xuan, R.-Y. Zhang, C.-H. Yang, X.-L. Song, Y.-D. Zhao, B. Liu, *Adv. Funct. Mater.* **2018**, *28*, 1803118.

[4] a) M. Valko, M. Izakovic, M. Mazur, C. J. Rhodes, J. Telser, *Mol. Cell. Biochem.* **2004**, *266*, 37-56; b) K. Dasuri, L. Zhang, J. N. Keller, *Free Radic. Biol. Med.* **2013**, *62*, 170-185; c) M. E. Goetz, A. Luch, *Cancer Lett.* **2008**, *266*, 73-83; d) B. A. Wagner, G. R. Buettner, C. P. Burns, *Biochemistry.* **1994**, *33*, 4449-4453.

[5] a) T. Finkel, N. J. Holbrook, *Nature* **2000**, *408*, 239-247; b) Y. Nosaka, A. Y. Nosaka, *Chem. Rev.* **2017**, *117*, 11302-11336.

[6] a) T. P. Szatrowski, C. F. Nathan, *Cancer Res.* **1991**, *51*, 794-798; b) M. López-Lázaro, *Cancer Lett.* **2007**, *252*, 1-8; c) Q. Chen, M. G. Espey, M. C. Krishna, J. B. Mitchell, C. P. Corpe, G. R. Buettner, E. Shacter, M. Levine, *P. Natl. Acad. Sci.* **2005**, *102*, 13604-13609; d) A. Gupte, R. J. Mumper, *Cancer Treat. Rev.* **2009**, *35*, 32-46.

[7] a) B. Yang, Y. Chen, J. Shi, *Chem. Rev.* **2019**, *119*, 4881-4985; b) D. Trachootham, J. Alexandre, P. Huang, *Nat. Rev. Drug Discov.* **2009**, *8*, 579-591; c) S. Kwon, H. Ko, D. G. You, K. Kataoka, J. H. Park, *Accounts. Chem. Res.* **2019**, *52*, 1771-1782.

[8] Z. Zhou, J. Song, L. Nie, X. Chen, *Chem. Soc. Rev.* **2016**, *45*, 6597-6626.

[9] a) B. Frei, S. Lawson, *P. Natl. Acad. Sci.* **2008**, *105*, 11037-11038; b) W. Yin, J. Yu, F. Lv, L. Yan, L. R. Zheng, Z. Gu, Y. Zhao, *ACS Nano* **2016**, *10*, 11000-11011; c) K. Fan, J. Xi, L. Fan, P. Wang, C. Zhu, Y. Tang, X. Xu, M. Liang, B. Jiang, X. Yan, L. Gao, *Nat. Commun.* **2018**, *9*, 1-11; d) S. Li, L. Shang, B. Xu, S. Wang, K. Gu, Q. Wu, Y. Sun, Q. Zhang, H. Yang, F. Zhang, L. Gu, T. Zhang, H. Liu, *Angew. Chem. Int. Edit.* **2019**, *58*, 12624-12631.

[10] L. -H. Fu, C. Qi, J. Lin, P. Huang, *Chem. Soc. Rev.* **2018**, *47*, 6454-6472.

[11] a) H. Tan, S. Guo, N. -D. Dinh, R. Luo, L. Jin, C. -H. Chen, *Nat. Commun.* **2017**, *8*, 663; b) W. Fan, N. Lu, P. Huang, Y. Liu, Z. Yang, S. Wang, G. Yu, Y. Liu, J. Hu, Q. He, J. Qu, T. Wang, X. Chen, *Angew. Chem. Int. Edit.* **2017**, *56*, 1229-1233; c) K. Chang, Z. Liu, X. Fang, H. Chen, X. Men, Y. Yuan, K. Sun, X. Zhang, Z. Yuan, C. Wu, *Nano. Lett.* **2017**, *17*, 4323-4329; d) J. Li, Y. Li, Y. Wang, W. Ke, W. Chen, W. Wang, Z. Ge, *Nano. Lett.* **2017**, *17*, 6983-6990; e) S. Wang, G. Yu, Z. Wang, O. Jacobson, L. -S. Lin, W. Yang, H. Deng, Z. He, Y. Liu, Z. -Y. Chen, X. Chen, *Angew. Chem.* **2019**, *131*, 14900-14905.

[12] S. Ma, J. Thiele, X. Liu, Y. Bai, C. Abell, W. T. S. Huck, *Small* **2012**, 8, 2356-2360.

[13] Q. Liu, Z. Yuan, M. Zhao, M. Huisman, G. Drewes, T. Piskorz, S. Mytnyk, G. J. M. Koper, E. Mendes, J. H. van Esch, *Unpublished Results.*

[14] a) S. Nagrath, L. V. Sequist, S. Maheswaran, D. W. Bell, D. Irimia, L. Ulkus, M. R. Smith, E. L. Kwak, S. Digumarthy, A. Muzikansky, P. Ryan, U. J. Balis, R. G. Tompkins, D. A. Haber, M. Toner, *Nature* **2007**, *450*, 1235-1239; b) P. Zhang, L. Chen, T. Xu, H. Liu, X. Liu, J. Meng, G. Yang, L. Jiang, S. Wang, *Adv. Mater.* **2013**, *25*, 3566-3570.

[15] Q. Liu, M. Zhao, S. Mytnyk, B. Klemm, K. Zhang, Y. Wang, D. Yan, E. Mendes, J. H. van Esch, *Angew. Chem. Int. Edit.* **2019**, *131*, 557-561.

[16] W. J. Luo, C. F. Zhu, S. Su, D. Li, Y. He, Q. Huang, C. H. Fan, *ACS Nano* **2010**, *4*, 7451-7458.

[17] J.-H. Oh, B. C. Kim, J.-S. Lee, *Anal. Bioanal. Chem.* **2014**, *406*, 7591-7600.

Entry for the Table of Contents

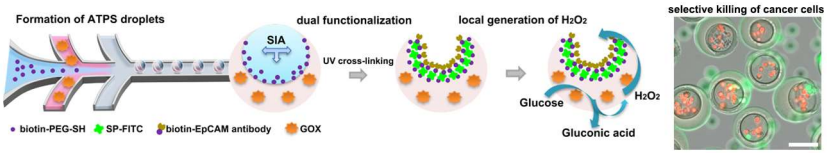

Dual-functionalized crescent microgels are designed and constructed by incorporating different functions within a single particle. These microgels are used for selectively capturing and killing cancer cells based on their high affinity to the lung cancer cells and local generation of high concentration of H_2O_2. It provides a novel strategy to create synergy in one unit for selective cancer chemotherapy.